

Synthesis, Structures, and Two-Photon Absorption Properties of Two New Heterocycle-Based Organic Chromophores

Yun-Xing Yan,*[1,2] Hai-Hua Fan,[1] Chi-Keung Lam,[1] Hong Huang,[1] Jing Wang,[1] Sheng Hu,[1] He-Zhou Wang,*[1] and Xiao-Ming Chen[1]

[1]State Key Laboratory of Optoelectronic Materials and Technologies, School of Chemistry and Chemical Engineering, Sun Yat-Sen University, Guangzhou 510275, P. R. China

[2]State Key Laboratory of Crystal Materials, Shandong University, Jinan 250100, P. R. China

Received March 29, 2006; E-mail: yxyan@icm.sdu.edu.cn

Two new heterocycle-based two-photon absorption chromophores, 4-[4-(4,5-diphenyl-1*H*-imidazol-2-yl)styryl]-pyridine (**2**) and (*E*)-4-{[2-(1*H*-benzimidazol-2-yl)vinyl]styryl}-*N*-methylpyridinium iodide (**4**), have been synthesized and characterized. The two molecules possess A–π–A′ structures. A π-deficient heteroaromatic ring (benzimidazole, 4,5-diphenyl-1*H*-imidazole) is used as an acceptor (A), and a pyridine ring is used as another acceptor (A′). One-photon-excited fluorescence, one-photon-fluorescence quantum yields, two-photon-excited fluorescence, and two-photon absorption cross-sections were investigated. Pumped with 740 and 800 nm laser excitation, compounds **2** and **4** had two-photon absorption cross-sections (41 and 38 GM) and two-photon-excited fluorescence (511 and 601 nm) in DMF, respectively. The crystal structure of compound **4** was determined by using X-ray single-crystal diffraction analysis.

Two-photon absorption (TPA) in organic molecules has attracted growing attention due to potential applications including microfabrication,[1–4] three-dimensional optical data storage,[5–8] optical power limitation,[9,10] localized photodynamic therapy,[11] and two-photon laser scanning fluorescence imaging.[12–14] These applications take advantage of the fact that the activity of two-photon absorption scales quadratically with the intensity of the incident laser radiation. Some of these applications are further based on the fluorescence properties of two-photon-excited molecules. In the case of two-photon-excited fluorescence (TPEF) microscopy, high-performance fluorophores must exhibit both high fluorescence quantum yields (Φ) and large two-photon absorption cross-sections (σ) in the near infrared region, corresponding to the biological optimal window for reduced photodamage. Photostability is also an important feature to consider for TPEF-based applications. To meet market criteria for these applications, molecules with large TPA cross-sections are required.

So far, the TPA activities of most dyes available are not large enough and lead to the use of either high laser intensity and/or high fluorophore concentration. To fully exploit the greater potential of TPA process, it is important to establish efficient methods for the synthesis of fluorophores that are amenable to further chemical functionalization or modification, which, in turn, can be expanded to obtain materials with large TPA cross-sections. In recent years, the optimization of molecular TPA has largely focused on one-dimensional dipolar[15–17] or quadrupolar structures,[18–26] and octupolar structures.[27–29] It should be pointed out that introducing a heteroatom into a molecular structure is another efficient way to obtain excellent TPEF molecules because π-deficient and π-excessive heterocycles may act as efficient acceptor and donor moieties, respectively.[24,30]

Recent studies showed that the heterocycle-based two-photon absorbing chromophores exhibit large TPA cross-sections. However, the mechanism and the fundamental structure–property relationships for increasing their TPA cross-sections are not completely clear. In this paper, we present the synthesis, structures, and TPA cross-sections of two new heterocycle-based organic chromophores, 4-[4-(4,5-diphenyl-1*H*-imidazol-2-yl)styryl]pyridine (**2**) and (*E*)-4-{[2-(1*H*-benzimidazol-2-yl)-vinyl]styryl}-*N*-methylpyridinium iodide (**4**). These two molecules have a general A–π–A′ structure. A π-deficient benzimidazole or 4,5-diphenyl-1*H*-imidazole is used as an acceptor (A), and the pyridine ring acts as a second acceptor (A′). These two molecules have strong one-photon-excited fluorescence (SPEF) and TPEF, and the experimental results showed that these two molecules are good TPA chromophores. The crystal structure of compound **4** was determined by X-ray single-crystal diffraction analysis (Scheme 1).

Experimental

Chemicals and Instruments. 1,4-Dimethylpyridinium iodide was synthesized according to the reported method.[31] 4-bromobenzaldehyde, benzil, 4-vinylpyridine (95%), and palladium(II) acetate (47.5% Pd) were purchased from Acros Organics. Tri-*o*-tolylphosphine was obtained from Tokyo Kasei Kogyo Co., Ltd. The ^{1}H NMR spectra were recorded at 300 MHz on a Mercury-Plus 300 spectrometer. Elemental analyses were performed by using Perkin-Elmer 2400 elemental analyzer. The melting points and decomposition temperatures were determined on a Netzsch DSC 204 thermal analyzer and a Netzsch TG 209 thermogravimetric analyzer at a heating rate of 10 °C min^{-1} under dinitrogen atmosphere, respectively. Mass spectra were measured on a LCMS-2010A liquid chromatograph mass spectrometer. UV–visible–near-IR spectra were measured on a UV-3150 spectrophotometer. The one-photon fluorescence spectra and quantum yields (Φ) were

Published on the web October 10, 2006; doi:10.1246/bcsj.79.1614

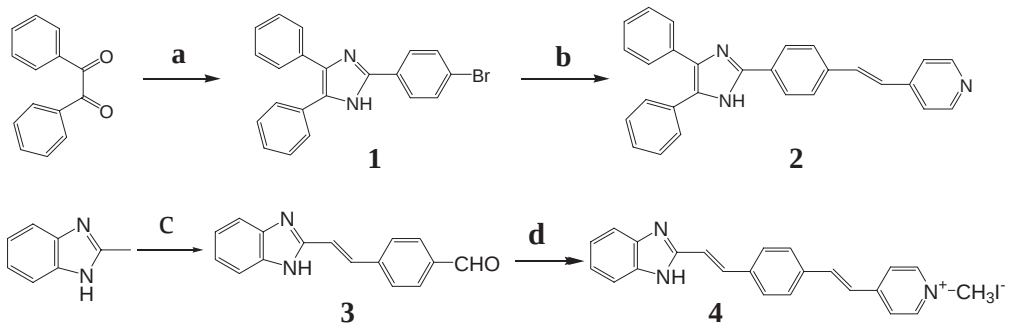

Scheme 1. Synthesis of compounds **2** and **4**: a) NH_4OAc/HOAc, reflux; b) 4-vinylpyridine/tri-*o*-tolylphosphine/palladium(II) acetate/triethylamine, reflux; c) $(Ac)_2O$/HOAc, 120 °C, 8 h; d) 1,4-dimethylpyridinium iodide/EtOH/piperidine, 80 °C, 12 h.

measured on a Hitachi F-4500 fluorescence spectrophotometer. Coumarin307 (whose Φ is assumed to be 56% in methanol) was used as the reference.[32] The concentration was the same as that of the linear absorption spectra. The path-length of the quartz cuvettes was 1 cm. The two-photon-induced fluorescence spectra were observed with a single sweep streak camera equipped with a polychromator as a recorder (Hamamatsu Model C1587). A mode-locked Nd:YAG laser (PC2143, pulse duration of 25 ps) was used to pump up the OPG (Optical Parameter Generator) system operating at 10 Hz, tuned from 420 to 10000 nm. The excitation wavelengths for compounds **2** and **4** were 740 and 800 nm, respectively. The concentrations are 1×10^{-3} mol L^{-1}, respectively.

Synthesis. 2-(4-Bromophenyl)-4,5-diphenyl-1*H*-imidazole (**1**). A mixture of benzil (1.05 g, 5 mmol), 4-bromobenzaldehyde (0.925 g, 5 mmol), ammonium acetate (2.5 g), and acetic acid (25 mL) was refluxed for 12 h and then cooled to room temperature. After adding concentrated hydrochloric acid (10 mL), the mixture was left for 1 h, filtered, and washed with water. The filtrate was treated with 30% aqueous sodium hydroxide solution (20 mL) to afford a pale-yellow precipitate. The crude product was purified by column chromatography on silica gel using ethyl acetate/petroleum ether (1:15) as eluent. Compound **1**, as a pale-yellow solid, obtained in 86% yield. Anal. calcd for $C_{21}H_{15}BrN_2$: C, 67.21; H, 4.03; N, 7.47%. Found: C, 66.94; H, 3.97; N, 7.36%. ^{1}H NMR (DMSO-d_6, 300 MHz) δ 8.11 (d, $J = 8.4$ Hz, 2H), 8.05 (s, 1H), 7.71 (d, $J = 8.4$ Hz, 2H), 7.48 (d, $J = 3.3$ Hz, 4H), 7.375 (d, $J = 3.3$ Hz, 6H). ESI-MS: m/z calcd for $C_{21}H_{15}BrN_2$ 374.04, found 374.15.

4-[4-(4,5-Diphenyl-1*H*-imidazol-2-yl)styryl]pyridine (**2**). Compound **1** (1.87 g, 5 mmol), tri-*o*-tolylphosphine (0.65 g, 2.15 mmol), 4-vinylpyridine (1.16 mL, 10.75 mmol), palladium(II) acetate (0.06 g, 0.27 mmol), and redistilled triethylamine (100 mL) under dinitrogen were added to a three-necked flask equipped with a magnetic stirrer, a reflux condenser, and a dinitrogen input tube. The reaction mixture was refluxed in an oil bath under dinitrogen. An orange product was obtained after heating and stirring for 24 h. Then, the solvent was removed under reduced pressure, and the residue was dissolved in dichloromethane, washed with distilled water (3 × 50 mL), and dried with anhydrous magnesium sulfate. The organic layer was filtered and concentrated. The resulting solution was chromatographed on silica gel using ethyl acetate/petroleum ether (1:1) as eluent. Compound **2** (mp 301.8 °C) was obtained as a yellow-green powder in a yield of 55%. The enthalpy is 126.2 mJ mg^{-1}. Anal. calcd for $C_{28}H_{21}N_3$: C, 84.18; H, 5.30; N, 10.52%. Found: C, 83.87; H, 5.32; N, 10.48%. ^{1}H NMR (DMSO-d_6, 300 MHz) δ 12.72 (s, 1H), 8.54 (d, $J = 5.1$ Hz, 2H), 8.11 (d, $J = 8.1$ Hz, 2H), 7.76 (d, $J = 8.1$ Hz, 2H), 7.44 (m, 14H). ESI-MS, m/z calcd for $C_{28}H_{21}N_3$ 399.17, found 399.25.

(*E*)-4-[2-(1*H*-Benzimidazol-2-yl)vinyl]benzaldehyde (**3**). Compound **3** was obtained according to the reported method,[30] and it was recrystallized from ethyl acetate to afford yellow crystals of compound **3** in 70% yield. Anal. calcd for $C_{16}H_{12}N_2O$: C, 77.40; H, 4.87; N, 11.28%. Found: C, 77.01; H, 4.79; N, 11.15%. ^{1}H NMR ($CDCl_3$, 300 MHz) δ 10.01 (s, 1H), 7.87 (d, $J = 8.4$ Hz, 2H), 7.69 (d, $J = 10.9$ Hz, 1H), 7.67 (s, 1H), 7.65 (d, $J = 5.9$ Hz, 1H), 7.62 (d, $J = 8.3$ Hz, 2H), 7.34 (d, $J = 3.3$ Hz, 1H), 7.31 (d, $J = 3.3$ Hz, 1H), 7.29 (d, $J = 7.0$ Hz, 2H).

(*E*)-4-{[2-(1*H*-Benzimidazol-2-yl)vinyl]styryl}-*N*-methylpyridinium iodide (**4**). At room temperature, (*E*)-4-[2-(1*H*-benzimidazol-2-yl)vinyl]benzaldehyde (1.24 g, 0.01 mol), 1,4-dimethylpyridinium iodide (1.18 g, 0.01 mol), ethanol (100 mL), and piperidine (three drops) were added to a one-neck flask (250 mL) equipped with a stirrer and a condenser. The mixture was refluxed for 8 h. After the solvent was removed, a red precipitate was obtained. The solid was recrystallized from ethanol, and orange-red crystals of compound **4** were obtained. The yield is 75% and decomposition temperature (T_d) is 295.8 °C. Anal. calcd for $C_{23}H_{20}IN_3 \cdot 2.5H_2O$: C, 54.12; H, 4.90; N, 8.23%. Found: C, 53.75; H, 4.82; N, 8.17%. ^{1}H NMR (DMSO-d_6, 300 MHz) δ 12.64 (s, 1H), 8.84 (d, $J = 6.6$ Hz, 2H), 8.21 (d, $J = 6.6$ Hz, 2H), 8.02 (d, $J = 16.2$ Hz, 1H), 7.79 (t, $J = 8.8$ Hz, 4H), 7.68 (d, $J = 16.5$ Hz, 1H), 7.49 (q, $J = 5.4$ Hz, 3H), 7.32 (d, $J = 16.5$ Hz, 1H), 7.18 (d, $J = 3.3$ Hz, 2H), 4.25 (s, 3H).

Crystallography. The X-ray diffraction data of compound **4** were collected on a Bruker Smart Apex CCD diffractometer (Mo Kα, $\lambda = 0.71073$ Å). An absorption correction was applied by using SADABS.[33] The structure was solved by direct methods and refined with a full-matrix least-squares analysis using SHELXS-97 and SHELXL-97 programs, respectively.[34,35] The ethylene groups with two-fold disorder (C7–C8, C30–C31, and C38–C39) were subjected to geometrical restraints in refinement. Anisotropic thermal parameters were applied to all non-hydrogen atoms. The organic hydrogen atoms were generated geometrically (C–H 0.96 Å); the hydrogen atoms except those on the water molecules were added geometrically and refined with isotropic temperature factors. Crystal data for $C_{23}H_{20}IN_3 \cdot 2.5H_2O$: Triclinic, space group $P\bar{1}$, $a = 9.706(2)$, $b = 13.588(3)$, $c = 18.244(3)$ Å, $\alpha = 75.821(3)$, $\beta = 79.282(3)$, $\gamma = 77.691(4)°$, M_r 505.32, $Z = 4$, $V = 2256.5(7)$ Å^3, $T = 293(2)$ K, $D_{calcd} = 1.487$ g cm^{-3}, $R_1 = 0.0514$, $wR_2 = 0.1059$ for 2467 reflections $I \geqq 2\sigma(I)$. CCDC reference number 610567.

Results and Discussion

Structure and Characterization. Selected bond lengths

Table 1. Selected Bond Lengths (Å) and Bond Angles (°) for Compound **4**

N1–C2	1.301(12)	C9–C8′	1.453(5)	C32–C37	1.422(15)
N1–C6	1.322(10)	C9–C8	1.464(5)	C32–C31	1.452(5)
N1–C1	1.482(10)	C10–C11	1.382(12)	C32–C31′	1.456(5)
N2–C17	1.297(10)	C11–C12	1.400(11)	C33–C34	1.356(12)
N2–C18	1.402(11)	C12–C13	1.376(11)	C34–C35	1.411(14)
N3–C17	1.395(10)	C12–C15	1.459(5)	C35–C36	1.390(15)
N3–C23	1.406(10)	C13–C14	1.394(11)	C35–C38′	1.452(5)
N4–C25	1.325(10)	C15–C16	1.315(5)	C35–C38	1.460(5)
N4–C29	1.350(11)	C16–C17	1.452(5)	C36–C37	1.375(13)
N4–C24	1.459(10)	C18–C19	1.387(12)	C40–C39	1.453(5)
N5–C41	1.347(10)	C18–C23	1.421(12)	C40–C39′	1.459(5)
N5–C40	1.397(14)	C19–C20	1.381(13)	C41–C42	1.393(11)
N6–C40	1.302(15)	C20–C21	1.345(14)	C41–C46	1.396(12)
N6–C46	1.348(12)	C21–C22	1.413(12)	C42–C43	1.384(12)
C2–C3	1.359(14)	C22–C23	1.397(11)	C43–C44	1.396(14)
C3–C4	1.367(15)	C25–C26	1.340(11)	C44–C45	1.337(14)
C4–C5	1.416(14)	C26–C27	1.379(17)	C45–C46	1.374(14)
C4–C7	1.455(5)	C27–C28	1.373(18)	C7–C8	1.313(5)
C4–C7′	1.458(5)	C27–C30′	1.450(5)	C7′–C8′	1.311(5)
C5–C6	1.334(12)	C27–C30	1.457(5)	C30–C31	1.309(5)
C9–C14	1.406(13)	C28–C29	1.362(14)	C38–C39	1.311(5)
C9–C10	1.445(14)	C32–C33	1.340(15)	C30′–C31′	1.311(5)
				C38′–C39′	1.308(5)
C2–N1–C6	120.7(9)	C22–C23–C18	122.3(9)	C37–C36–C35	120.8(12)
C17–N2–C18	105.7(8)	N3–C23–C18	104.1(9)	C36–C37–C32	120.9(11)
C17–N3–C23	106.6(8)	N4–C25–C26	122.0(10)	N6–C40–N5	108.5(8)
N1–C2–C3	121.2(11)	C25–C26–C27	124.3(12)	C41–N5–C40	110.0(9)
C2–C3–C4	121.6(11)	C25–N4–C29	118.1(9)	C40–N6–C46	107.0(10)
C3–C4–C5	114.3(9)	C28–C27–C26	110.8(10)	N5–C41–C46	102.6(9)
C19–C18–C23	121.2(10)	C28–C27–C30′	100.0(16)	C42–C41–C46	123.2(10)
N2–C18–C23	110.2(9)	C29–C28–C27	126.0(13)	C43–C42–C41	115.2(9)
C20–C19–C18	116.8(11)	N4–C29–C28	118.7(11)	C42–C43–C44	120.9(10)
C21–C20–C19	121.0(12)	C33–C32–C37	116.3(10)	C45–C44–C43	123.0(11)
C20–C21–C22	126.0(11)	C32–C33–C34	125.0(12)	C44–C45–C46	118.3(12)
C23–C22–C21	112.6(10)	C33–C34–C35	119.2(11)	N6–C46–C41	111.8(10)
C22–C23–N3	133.5(11)	C36–C35–C34	117.7(10)	C45–C46–C41	119.4(12)

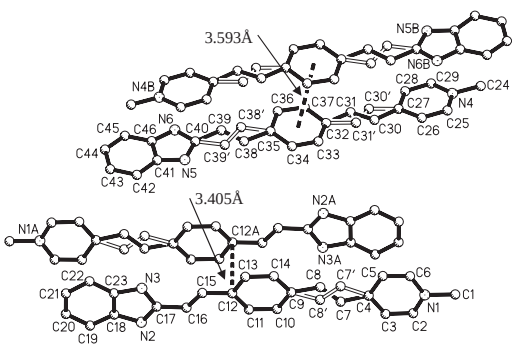

Fig. 1. Perspective views of π–π stacking interactions (dash line) in compound **4**. Symmetry codes: A($-1-x$, $3-y$, $2-z$) and B($-1-x$, $3-y$, $1-z$).

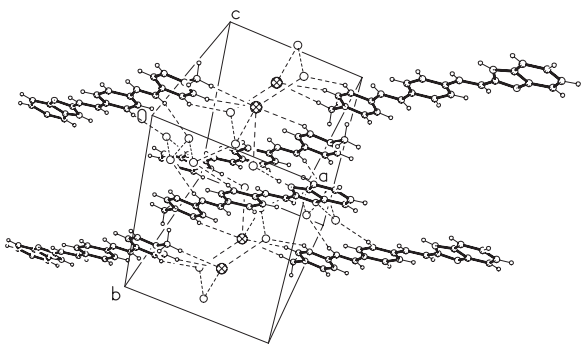

Fig. 2. Hydrogen-bonding interactions in compound **4**.

and bond angles of compound **4** are summarized in Table 1. The molecular structure and packing diagram are depicted in Figs. 1 and 2, respectively.

There are two crystallographically independent organic cations in the asymmetric unit. All of their bond lengths lie in the usual range. The organic cations in the crystal structure of compound **4** are conjugated and essentially planar. In one of the crystallographically independent organic cations, the dihedral angle between the benzimidazole and phenyl rings is 6.3°, and that between the phenyl and pyridinium rings is 10.0°. For the other crystallographically independent organic cation, the dihedral angle between the benzimidazole and phenyl rings is 7.5°, and that between the phenyl and pyridinium rings is 10.5°. Therefore, compound **4** is a highly delocalized π-elec-

tron system, which is a necessary structural characteristic for two-photon absorption.

Lattice water molecules are found to be co-crystallized in the crystal structure of compound **4**, forming various hydrogen bonds, such as the O–H···N hydrogen bond between a water molecule and a benzimidazole group, the O–H···I^- hydrogen bond between a water molecule and an iodide ion, the N–H···I^- hydrogen bond between a benzimidazole group and an iodide ion, the O–H···O hydrogen bond among the water molecules. Some interesting phenomena were also observed, Fig. 3. Hydrogen-bonded hexagons are formed by O1w, O2w, I^-, and their centrosymmetrically related partners. Apart from strong hydrogen-bonding interactions, other weak intermolecular interactions, such as aromatic π–π interactions between conjugated organic cations, are also found in the crystal structure of compound **4**. The two different organic cations are orientated in different directions and stacked in a head-to-tail fashion. The inter-planar distances are 3.405 and 3.593 Å, respectively, indicating strong π–π interactions between adjacent organic cations (Fig. 1).

One- and Two-Photon Fluorescence. The photophysical properties of the two compounds are summarised in Table 2. The linear absorption, one-photon fluorescence, and two-photon fluorescence spectra in DMF are shown in Fig. 4. The linear absorption spectra were measured in solvents of different polarity at a concentration of 1×10^{-5} mol L^{-1}, in which the solvent influence has been excluded. Figure 4 shows that the solutions of compounds **2** and **4** in DMF are completely transparent above 500 nm. The one-photon fluorescence spectra were measured with the same concentrations as those of the linear absorption spectra, and excitation wavelengths for compounds **2** and **4** are 385 and 435 nm, respectively.

As shown in Table 2, the absorption maxima are not significantly different, although the one- and two-photon fluorescence maxima are slightly red-shifted, and the fluorescent lifetimes are lengthened upon increasing the polarity of the aprotic solvent for compound **2**. This fact can be attributed to the fact that the excited states may have a higher polarity than that of the ground state, since solvatochromism is associated with the lowering of energy levels. By increasing dipole–dipole interactions between the solute and solvent, the energy level can be lowered greatly.[36,37] In the case of ethanol, the fluorescence maximum is slightly red-shifted compared to those in other aprotic solvents. The formation of hydrogen bonds between the solvent and solute molecules also lowers the excitation energy.[38] The absorption and one-photon fluorescence maxima for compound **4** show a similar trend upon increasing the polarity of solvent except ethanol.

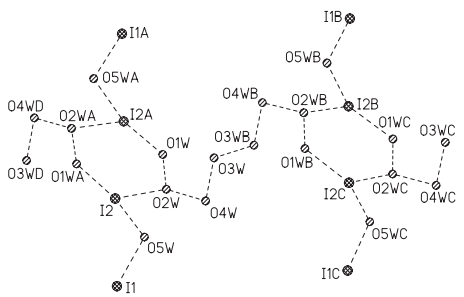

Fig. 3. Hydrogen-bonding interactions between iodide ions and water molecules in compound **4**. Symmetry codes: A($1-x, 2-y, 1-z$), B($2-x, 1-y, 1-z$), and C($1-x, y-1, z$).

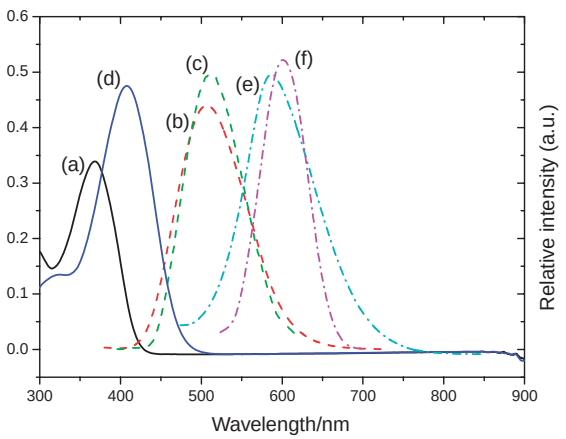

Fig. 4. Absorption and fluorescence spectra of compounds **2** and **4** in DMF: linear absorption (a), one- (b) and two-photon (c) fluorescence spectra of compound **2**; linear absorption (d), one- (e) and two-photon (f) fluorescence spectra of compound **4**.

Table 2. The Data of Absorption, One- and Two-Photon Fluorescence with Solvent Effects of Compounds **2** and **4**[a)]

Compds	Solvents	$\lambda_{max}^{(1a)}$/nm	$\varepsilon_{res}/10^4$	$\lambda_{max}^{(1f)}$/nm	$\Delta\nu$/cm^{-1}	τ/ns	Φ/%	$\lambda_{max}^{(2)}$/nm
2	DMF	368	3.39	507	7450	3.16	59	511
	Ethyl acetate	357	3.20	490	7603		78	
	Ethanol	360	3.50	510	8170		54	
	THF	365	3.38	490	6989	2.53	72	494
	$CHCl_3$	355	2.70	484	7508	2.03	78	487
	Toluene	357	2.43	479	7134		90	
4	DMF	408	4.75	586	7445	0.08	0.73	601
	Ethyl acetate	395	1.84	581	8104		5.23	
	Ethanol	407	5.02	578	7269		1.52	
	THF	392	2.41	571	7997		3.50	
	$CHCl_3$	410	1.62	565	6691		1.18	

a) $\lambda_{max}^{(1a)}$, $\lambda_{max}^{(1f)}$, and $\lambda_{max}^{(2)}$ are one-photon absorption, one-photon fluorescence, and two-photon fluorescence peak maxima, respectively. Φ is one-photon fluorescence quantum yield determined using coumarin 307 as the standard.[32] τ is two-photon fluorescence lifetime. $\Delta\nu$ is Stokes' shift. ε_{res} is the corresponding molar absorption coefficient.

By comparing Table 2 and Fig. 4, we can see that the two-photon fluorescence maxima of compound **2** do not shift compared to the corresponding one-photon fluorescence maxima in the same solvent. Although the two-photon fluorescence spectra are measured at concentrations, higher than those need to measure the one-photon fluorescence spectra, the Stokes' shift is large enough to make re-absorption effects negligible.[39] As shown in Fig. 4, there is no obvious overlap between the blue side of the one-photon-induced fluorescence band and the red side of the linear absorption band. For compound **4**, the two-photon fluorescence maximum has red-shifted compared to the one-photon fluorescence maximum in DMF. This can be ascribed to the effect of re-absorption for the linear absorption band which slightly overlaps the emission band and to the high concentrations in the two-photon fluorescence experiments that made re-absorption significant. By considering the similarities between SPEF and TPEF, we can conclude that, although the molecules can be excited to different excited states by one-photon absorption or two-photon absorption due to the different spectral selection rules, they finally relax to the same fluorescent excited state. It is clear that structural and environmental factors influence the SPEF and TPEF properties.

The TPA Cross-Section. The TPA σ of the two molecules were determined by comparing their TPEF with the two-photon fluorescence excitation σ of Rhodamine 6G (at a concentration of 5×10^{-4} mol L^{-1} in methanol) according to the following equation:[40]

$$\sigma_s = \sigma_r \frac{\Phi_r}{\Phi} \frac{c_r}{c} \frac{n_r}{n} \frac{F_s}{F_r}, \quad (1)$$

where the subscripts s and r refer to the sample and the reference material, and the terms c and n are the concentration and refractive index of the sample solution, respectively. Φ is the fluorescence quantum yield, F is two-photon-excited fluorescence integral intensity, and σ_r is the TPA cross-section of the reference molecule.

The excitation wavelengths of compounds **2** and **4** are 740 and 800 nm, respectively. The concentration was 1×10^{-3} mol L^{-1}. The two-photon cross-sections for rhodamine 6G are 21 and 35 GM at 740 and 800 nm, respectively.[41] The TPA cross-sections of compounds **2** and **4** are 41 and 38 GM, respectively. However, it should be noted that the optimal excitation wavelength for the TPA should be slightly less than two times of the wavelength for the linear absorption maxima.[42] A significant increase in the TPA cross-section value is expected at the optimal excitation wavelength for TPA.

Conclusion

In summary, two new heterocycle-based two-photon absorption chromophores have been synthesized and characterized. The crystal structure of compound **4** was determined by X-ray single-crystal diffraction analysis, and showed that compound **4** has a planar structure that contributes to the two-photon absorption. These two molecules exhibit strong one- and two-photon fluorescence. Moreover, chromophore **2** shows excellent thermal stability, one-photon fluorescence quantum yields, and long two-photon fluorescent lifetimes. These results indicate that chromophore **2** is a good two-photon absorbing chromophore and can be used in nonlinear optical materials.

This work was supported by NSFC (Nos. 20531070, 50323006, and 50402018), Guangdong Provincial Science and Technology Bureau (No. 04205405) and China Postdoctoral Science Foundation (No. 2004036515).

References

1 M. Saruo, O. Nakamura, S. Kawata, *Opt. Lett.* **1997**, *22*, 132.

2 B. H. Cumpston, S. P. Ananthavel, S. Barlow, D. L. Dyer, J. E. Ehrlich, L. L. Erskine, A. A. Keikal, S. M. Kuebler, I.-Y. S. Lee, D. M. Maughon, J. Qin, H. Röckel, M. Rumi, X. L. Wu, S. R. Marder, J. W. Perry, *Nature* **1999**, *398*, 51.

3 S. Kawata, H.-B. Sun, T. Tanaka, K. Takada, *Nature* **2001**, *412*, 697.

4 W. Zhou, S. M. Kuebler, K. L. Braun, T. Yu, J. K. Cammack, C. K. Ober, J. W. Perry, S. R. Marder, *Science* **2002**, *296*, 1106.

5 D. A. Parthenopoulos, P. M. Rentzepis, *Science* **1989**, *245*, 843.

6 J. H. Strickler, W. W. Webb, *Opt. Lett.* **1991**, *16*, 1780.

7 A. S. Dvornikov, P. M. Rentzepis, *Opt. Commun.* **1995**, *119*, 341.

8 K. D. Belfield, Y. Liu, R. A. Negres, M. Fan, G. Pan, D. J. Hagan, F. E. Hernandez, *Chem. Mater.* **2002**, *14*, 3663.

9 G. S. He, G. C. Xu, P. N. Prasad, B. A. Reinhardt, J. C. Bhatt, A. G. Dillard, *Opt. Lett.* **1995**, *20*, 435.

10 J. E. Ehrlich, X. L. Wu, I.-Y. S. Lee, Z.-Y. Hu, H. Röckel, S. R. Marder, J. W. Perry, *Opt. Lett.* **1997**, *22*, 1843.

11 J. D. Bhawalkar, N. D. Kumar, C. F. Zhao, P. N. Prasad, *J. Clin. Laser Med. Surg.* **1997**, *15*, 201.

12 W. Denk, J. H. Strickler, W. W. Webb, *Science* **1990**, *248*, 73.

13 C. Xu, W. R. Zipfel, J. B. Shear, R. M. William, W. W. Webb, *Proc. Natl. Acad. Sci. U.S.A.* **1996**, *93*, 10763.

14 D. R. Larson, W. R. Zipfel, R. M. Williams, S. W. Clark, M. P. Bruchez, F. W. Wise, W. W. Webb, *Science* **2003**, *300*, 1434.

15 K. D. Belfield, D. J. Hagan, E. W. Van Stryland, K. J. Schafer, R. A. Negres, *Org. Lett.* **1999**, *1*, 1575.

16 K. D. Belfield, K. J. Schafer, W. Mourad, B. A. Reinhardt, *J. Org. Chem.* **2000**, *65*, 4475.

17 A. Abbotto, L. Beverina, R. Bozio, S. Bradamante, C. Ferrante, G. A. Pagani, R. Signorini, *Adv. Mater.* **2000**, *12*, 1963.

18 Y.-X. Yan, X.-T. Tao, Y.-H. Sun, C.-K. Wang, G.-B. Xu, W.-T. Yu, H.-P. Zhao, J.-X. Yang, X.-Q. Yu, Y.-Z. Wu, X. Zhao, M.-H. Jiang, *New. J. Chem.* **2005**, *29*, 479.

19 O.-K. Kim, K.-S. Lee, H. Y. Woo, K.-S. Kim, G. S. He, S. H. Guang, J. Swiatkiewicz, P. N. Prasad, *Chem. Mater.* **2000**, *12*, 284.

20 Y.-X. Yan, X.-T. Tao, Y.-H. Sun, G.-B. Xu, C.-K. Wang, J.-X. Yang, X. Zhao, M.-H. Jiang, *J. Solid State Chem.* **2004**, *177*, 3007.

21 Y.-X. Yan, X.-T. Tao, Y.-H. Sun, W.-T. Yu, G.-B. Xu, C.-K. Wang, J.-X. Yang, X. Zhao, M.-H. Jiang, *Bull. Chem. Soc. Jpn.* **2005**, *78*, 300.

22 M. Albota, D. Beljonne, J.-L. Brédas, J. E. Ehrlich, J.-Y. Fu, A. A. Heikal, S. E. Hess, T. Kogej, M. D. Levin, S. R. Marder, D. McCord-Maughon, J. W. Perry, H. Röckel, M. Rumi, G. Subramaniam, W. W. Webb, X.-L. Wu, C. Xu, *Science* **1998**, *281*, 1653.

23 P. K. Frederiksen, M. Jørgensen, P. R. Ogilby, *J. Am.*

Chem. Soc. **2001**, *123*, 1215.
24 A. Abbotto, L. Beverina, R. Bozio, A. Facchetti, C. Ferrante, G. A. Pagani, D. Pedron, R. Signorini, *Org. Lett.* **2002**, *4*, 1495.
25 W. J. Yang, D. Y. Kim, M.-Y. Jeong, H. M. Kim, S.-J. Jeon, B. R. Cho, *Chem. Commun.* **2003**, 2618.
26 S. J. K. Pond, M. Rumi, M. D. Levin, T. C. Parker, D. Beljonne, M. W. Day, J.-L. Brédas, S. R. Marder, J. W. Perry, *J. Phys. Chem. A* **2002**, *106*, 11470.
27 S.-J. Chung, K.-S. Kim, T.-C. Lin, G. S. He, J. Swiatkiewicz, P. N. Prasad, *J. Phys. Chem. B* **1999**, *103*, 10741.
28 Y.-X. Yan, X.-T. Tao, Y.-H. Sun, C.-K. Wang, G.-B. Xu, J.-X. Yang, Y. Ren, X. Zhao, Y.-Z. Wu, X.-Q. Yu, M.-H. Jiang, *J. Mater. Chem.* **2004**, *14*, 2995.
29 D. Beljonne, W. Wenseleers, E. Zojer, Z. Shuai, H. Vogel, S. J. K. Pond, J. W. Perry, S. R. Marder, J.-L. Brédas, *Adv. Funct. Mater.* **2002**, *12*, 631.
30 Z.-L. Huang, H. Lei, N. Li, Z.-R. Qiu, H.-Z. Wang, J.-D. Guo, Y. Luo, Z.-P. Zhong, X.-F. Liu, Z.-H. Zhou, *J. Mater. Chem.* **2003**, *13*, 708.
31 C. F. Zhao, G. S. He, J. D. Bhawalkar, C. K. Park, P. N. Prasad, *Chem. Mater.* **1995**, *7*, 1979.
32 J. N. Demas, G. A. Crosby, *J. Phys. Chem.* **1971**, *75*, 991.
33 R. Blessing, *Acta Crystallogr., Sect. A* **1995**, *51*, 33.
34 G. M. Sheldrick, *SHELXS-97, Program for Crystal Structure Solution*, Göttingen University, Germany, **1997**.
35 G. M. Sheldrick, *SHELXL-97, Program for Crystal Structure Refinement*, Göttingen University, Germany, **1997**.
36 P. Fromherz, *J. Phys. Chem.* **1995**, *99*, 7188.
37 U. Narang, C. F. Zhao, J. D. Bhawalkar, F. V. Bright, P. N. Prasad, *J. Phys. Chem.* **1996**, *100*, 4521.
38 C.-K. Wang, P. Macak, Y. Luo, H. Ågren, *J. Chem. Phys.* **2001**, *114*, 9813.
39 G. S. He, L. Yuan, Y. Cui, M. Li, P. N. Prasad, *J. Appl. Phys.* **1997**, *81*, 2529.
40 Z.-Q. Liu, Q. Fang, D. Wang, D.-X. Cao, G. Xue, W.-T. Yu, H. Lei, *Chem. Eur. J.* **2003**, *9*, 5074.
41 M. A. Albota, C. Xu, W. W. Webb, *Appl. Opt.* **1998**, *37*, 7352.
42 C. Xu, R. M. Williams, W. Zipfel, W. W. Webb, *Bioimaging* **1996**, *4*, 198.